GRAVL: GRAvity observations by Vertical Laser ranging

N. Anthony, M. Archimbaud, S.S. Beeck, I. Bjorge-Engeland, E. Bogacz, V. Camplone, M. Eizinger, V. Galetsky, M. Noeker, L. Salfenmoser, E.A. Savu, M. Stefko, E.F.M. Weterings, A.J.P. Woodwark and R. Zeif

Tutors: Q. Chen and J. Praks

Team Green, Alpbach Summer School 2019 July 16–25, Alpbach/Tyrol — Austria

"They did not know it was impossible so they did it."
– Mark Twain

Abstract

We propose a mission to study mass redistribution in the upper mantle before, during, and after earthquakes by measuring the vertical component of the gravity vector of low-orbiting satellites from a high-orbit laser ranging platform. The processes behind solid-Earth mass movements and ocean water redistribution caused by earthquakes are poorly understood, due to the limited capabilities of terrestrial measurement systems. A well-proven alternative is to study gravitational anomalies from space; previous space based gravity missions have demonstrated detection of earthquakes with magnitudes larger than M_W 8.3 [1]. We propose a mission to extend the range of earthquake magnitudes observable from space to M_W 6.5. In order to achieve this goal, it is necessary to measure anomalies in Earth's gravitational field with a spatial resolution of 100 km every 3 days. This can be achieved by measuring the vertical deviations of twelve satellites in Low-Earth Orbit (LEO) from three platforms in Geostationary Orbit (GEO) with a laser. These measurements can be combined with telemetry data from the LEO satellites to build a model of the changes in Earth's mass distribution. This mission also contributes to the knowledge of silent earthquakes, in addition to filling gaps in locations where measurement data is currently lacking. The total cost of this mission is estimated around 380 million Euro.

1 Scientific Background

1.1 Earthquakes

Earthquakes are often defined as ground vibrations related to the sudden release of elastic energy, which creates seismic waves. During one year, there are about one million earthquakes, but only a few thousand of them are strong enough to be felt on the surface. When earthquakes occur in inhabited areas, they cause serious damage to infrastructure and result in significant injuries and death.

The majority of earthquakes occur along plate boundaries, and abnormally large earthquakes often happen in subduction zones (Figure 1). Earthquakes manifest themselves almost exclusively within certain bands of the Earth's surface, the seismically active areas. The general distribution of the seismic bands coincides with the location of large mountain ranges, oceanic ridges and other topographic and bathymetric features.

Some earthquakes do not create seismic waves, known as silent earthquakes, exhibiting low perturbations, typically having magnitudes between 6 and 7 [5]. We are thus looking for a sensitivity of M_W 6.5 in order to observe some of them. Silent earthquakes can lead to more damaging seismic events as they cause undetected stresses on fault lines.

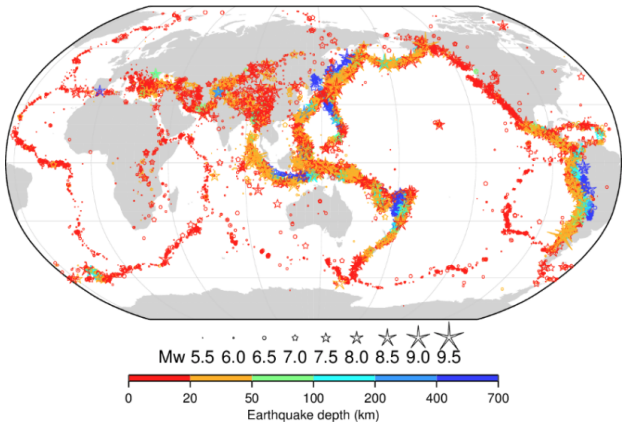

Figure 1: *Global overview of earthquakes listed in the Version 6.0 of the ISC-GEM Catalogue [2]. Symbols according to Agnew [3] with method as described by Bondár [4]. Most earthquakes appear between a rough latitude band of $\pm 60°$. Clear geophysical and tectonic features like the mid-ocean ridge and the pacific "Ring of Fire" are clearly correlated to the occurrence of seismic events.*

1.2 Monitoring Earthquakes with Space-borne Gravimetry

Conventionally, monitoring seismic processes uses sensitive seismographs to record the ground motion from seismic waves created by earthquakes. This approach does however have some limitations. Ground-based stations are sparsely distributed, and it is also very challenging to install ocean-bottom seismometers whilst maintaining a high degree of accuracy. Scientists also use gravimeters to measure small changes in the Earth's gravity field close to seismic events, though they suffer from similar limitations.

With the advent of space based observations, remote sensing techniques like InSAR (Interferometric Synthetic Aperture Radar) are adopted to identify and monitor seismic phenomena that produce surface deformations. These techniques are limited to detecting only crustal displacement at the Earth's surface, and are not able to detect mass movements happening in the subsurface of the Earth.

The GOCE (Gravity Field and Steady-State Ocean Circulation Explorer, 2009-2013) mission [6] consisted of a single spacecraft, carried six accelerometers, flew at low altitudes, which allowed for the retrieval of the static gravitational field at a high spatial resolution of 100 km and sensitivity of 1 mGal. In contrast, the GRACE (Gravity Recovery and Climate Experiment, 2002-2017) [7] and GRACE Follow-On missions (2018-present) have performed along-track microwave ranging to detect deviations from the expected orbits of two spacecrafts. It was possible to reach a higher sensitivity (up to 1 μGal) at lower spatial resolution, around 300 km, which provided opportunities to detect gravity signatures caused by large earthquakes [8]. However, its relatively low sensitivity and spatial resolution enables the detection of earthquakes with magnitudes above M_W 8.3 [1]. In addition, an understanding of the mechanisms and timescales of far-field motions leading to seismic events remains challenging. An important limitation comes from an incomplete description of seismic mass fluxes at depth along plate boundaries [9]. A future mission with higher spatial resolution would provide significant benefits.

Therefore, concepts for gravity measurements from space have been and currently are under investigation. For instance, the NGGM (Next Generation Gravity Mission) concept of a GRACE-like mission with an additional satellite pair at different inclination is under investigation [10]. Other concepts are GETRIS [11] and MOBILE [12], which proposed constellations that use high precision, high–low inter-satellite links to measure the radial distance between spacecraft orbiting the Earth at different altitudes.

2 Scientific Objectives

2.1 Primary Science Objective

Improving both spatial and temporal resolution to 100 km and 3 days, and the Earth's gravity field to a precision of 0.1 μGal will provide the basis for an improved understanding of the geophysical pre-, co- and post-processes governing seismic events. Such understanding will not only improve the understanding of these often devastating events, possibly contributing to eventually achieving predictability, but also the interior of our planet. The upper mantle's rheology is not very well understood; however, it can be derived from mass displacement observations. According to Panet [8], better constraints on the rheology of the crust and mantle can provide a wealth of geophysical information. Here, one of the least understood and most important parameters is the mantle viscosity. A better understanding of this parameter will improve the understanding of the dynamics inside the mantle and the behaviour of convective flows. By gathering data on silent earthquakes, understanding of these rare and long-timescale events is improved. Finally, knowledge of mass movement associated with seismic events in areas with currently sparse coverage by ground measurement networks is improved, especially addressing inaccessible areas such as the oceans.

2.2 Secondary Science Objectives

Improving the spatial resolution also enables a better understanding of ocean currents, including how they are affected by climate change. It can also improve understanding of the hydrological cycle.

Changes in the Earth's water storage distribution cause variations in the Earth's gravity field [13]. As an

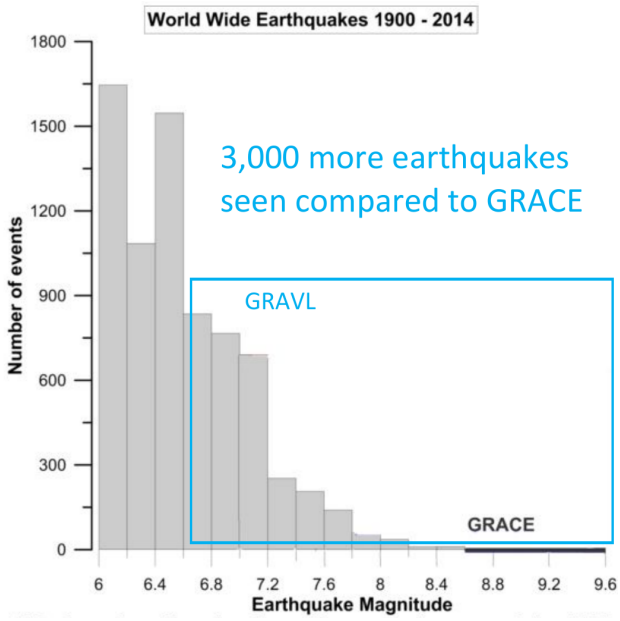

Figure 2: *Global M_W distribution of earthquakes between 1900 and 2014. Seismic events that can be resolved by GRACE, the minimum success criterion (M_W 7.0) and the science goal (M_W 6.5) are indicated. Figure adapted from Visser [14].*

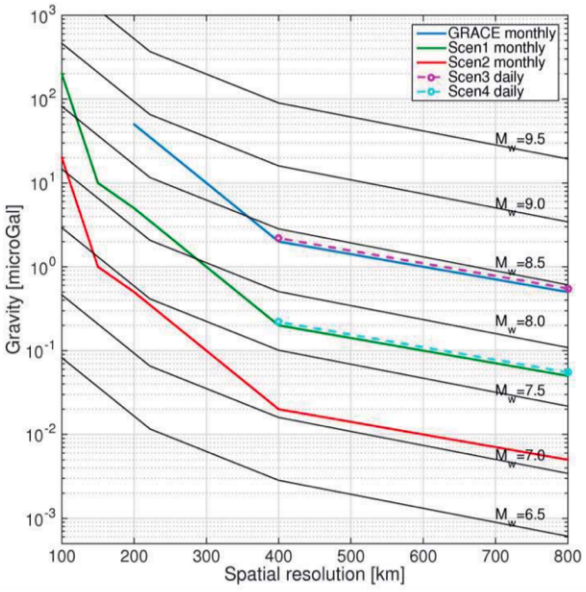

Figure 3: *Relationship between spatial resolution, sensitivity of gravity measurement, and observable seismic event magnitude [13].*

example, the Atlantic Meridional Overturning Circulation (AMOC) is a collection of large ocean currents that plays a key role in regulating the Earth's climate. Ice melting in the North Atlantic Ocean may slow this process down or eventually even cause its stop completely. Proper, long-time monitoring of the AMOC would help in understanding its response to climate change.

The hydrological cycle is the succession of the phenomena of flow and circulation inside the terrestrial hydrosphere, and the changes in its physical state (liquid, gaseous and solid). It refers to the continuous exchange of water mass between different areas of the Earth: ocean bodies, various surface waters and groundwater. Gravity measurements with improved spatial resolution would allow for the monitoring of water storage changes in not only the large river basins, but also smaller ones [13].

3 Scientific and Engineering Requirements

3.1 Observational Requirements

To be able to observe a reasonable amount of earthquakes, and silent earthquakes, a threshold of M_W 6.5 is chosen (Figure 2). As shown in Figure 3, the GRACE mission provided measurements that allowed the resolution of mass redistribution of seismic events down to M_W 8.3. To be able to observe earthquakes of the specified threshold, the spatial resolution and sensitivity must be chosen accordingly. Therefore, a spatial resolution of 100 km and sensitivity of 0.1 μGal have been used.

A 1-day evenly distributed coverage with low accuracy (1 μGal) is chosen to be able make observations on a timescale where short term gravitational anomalies occur, and allow these high frequency signals to be accounted for in processing. After a 3-days coverage a higher accuracy is obtained and the coverage repeats.

In addition, silent earthquakes statistically occur every 13 to 16 months in the region of British Columbia, which is between 50° and 60° latitude [15]. Therefore, a coverage between $\pm$60° latitude is required. Importantly, the selected coverage includes 98 % of earthquakes with magnitudes greater than M_W 6.5.

Nevertheless, the duration of the mission is planned for 7 years, as there is a 99 % probability that at least one silent earthquake will occur within that time period. It also improves the chance that we will be able to observe both, a few years before and after an earthquake.

3.2 Measurement Concept

In order to fulfil the observational requirements, we propose a system where accurate distance and location measurements of a global small satellite constellation on LEO is conducted by combining laser ranging measurements between GEO and LEO spacecraft with accurate location measurements and acceleration measurements of both spacecraft. This configuration allows measurement of distance changes aligned with gravity field radial components, directly accessing the largest component of the field. In this configuration, the required sampling density is achieved by using sufficient

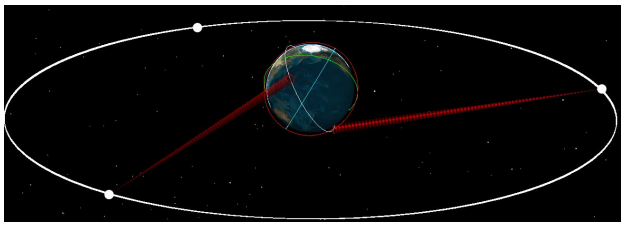

Figure 4: *Observation configuration. 3 GEO satellites equally spaced around the Earth regularly measure the distance to 12 LEO spacecraft using laser time-of-flight measurements.*

amounts of LEO satellites in the LEO constellation (Figure 4).

3.3 Instrument Requirements

3.3.1 Laser Ranging Requirements

In LEO and GEO the spacecraft (s/c) will experience perturbational forces. These accelerations shall be measured with sufficient accuracy. The LEO satellite therefore requires a very precise accelerometer, gyroscope and star tracker. The position and orientation of the retro-reflector can be calculated and is included in the distance analysis. The LEO s/c will experience drag, which guarantees re-entry of the spacecraft and meets space debris mitigation requirements. To account for drag forces in the gravity field computation, a highly accurate accelerometer is required. In GEO there is no drag, but there are still perturbations. This will also be corrected by an accelerometer, gyroscope and star tracker.

3.3.2 Correction of Non-gravitational Forces

In LEO, atmospheric drag is the predominant perturbing force acting on the s/c. Radiation pressure is here generally weaker but cannot be neglected to achieve the high precision measurements required for this gravity mission. In this subsection, the instrument requirement is derived from calculated drag and radiation pressure accelerations. In general, atmospheric drag is much harder to model than radiation pressure due to the uncertainties of the atmosphere's movement and density at large altitudes.

The atmospheric drag acceleration a_{drag} acting on an orbiting spacecraft is calculated as:

$$a_{drag} = -\frac{1}{2}\rho||v - v_{atm}||(v - v_{atm})C_D\frac{A}{m}, \qquad (1)$$

where the ballistic coefficient $B = C_D\frac{A}{m}$ comprises of the satellite's drag coefficient C_D, the effective cross-section A, and the satellite mass m. ρ is the atmospheric density at the orbits altitude, and $||v - v_{atm}||$ is the s/c velocity relative to the atmosphere. Only for very small separations of ca. 10 km, but not for GRACE or SWARM separations (ca. 200 km), a simplification can be made that the atmospheric density is identical for both s/c, e.g. Gaias [16]. To select the accelerometer required to correct for atmospheric perturbation, the density for an altitude of 500 km is obtained from The Committee on Space research (COSPAR) [17] with a density range between low ($6.79 \cdot 10^{-14}$ kg/m^3) and high ($3.76 \cdot 10^{-12}$ kg/m^3) solar and geomagnetic activities. With a very good ballistic coefficient $B = 0.008$ m^2/kg of the spherical spacecraft (Section 5.3), the atmospheric perturbing acceleration is calculated as shown in Table 1.

Table 1: *Estimated drag perturbing acceleration in ms^{-2} for spherical LEO s/c (d=0.5 m) at 500 km orbital altitude.*

low activity	mid activity	high activity
$1.547 \cdot 10^{-8}$	$1.788 \cdot 10^{-7}$	$8.566 \cdot 10^{-7}$

Furthermore, the radiation pressure perturbation has been quantified for geosynchronous and low-Earth orbit designs as shown in Table 2.

Table 2: *Radiation acceleration for both GEO and LEO designs per satellite.*

Orbit	a_{rad} [ms^{-2}]
LEO	$2.45 \cdot 10^{-8}$
GEO	$5.14 \cdot 10^{-8}$

The above results have been obtained with Equation (2) according to Wakker [18]:

$$a_{rad} = \frac{C_R W A}{Mc}, \qquad (2)$$

where C_R is the satellite's reflectivity (0.68), W is the mean solar radiation flux (1366 Wm^{-2}), A is the effective cross-sectional area of the satellite normal to the solar vector and M is the mass of the satellite.

Overall, the calculated radiation acceleration is smaller than the drag acceleration at mid and high solar and geomagnetic activities. Yet it cannot be neglected in this mission scenario as it would induce a significant error in the orbit reconstruction leading to errors in the gravity field reconstruction. In order to correct for these effects, an acceleration of at least 1 nm/s ^{2} must be achieved.

4 Mission Design

The following subsections discuss the mission requirements, which are derived from the science and observation requirements. The mission requirements affect the orbit design for both LEO and GEO satellites.

4.1 Orbit Design and Manoeuvres

The orbital design was mainly driven by the observation requirements which occur with a temporal resolution of 3 days, a spatial resolution of 100 km, and a lifetime of seven years.

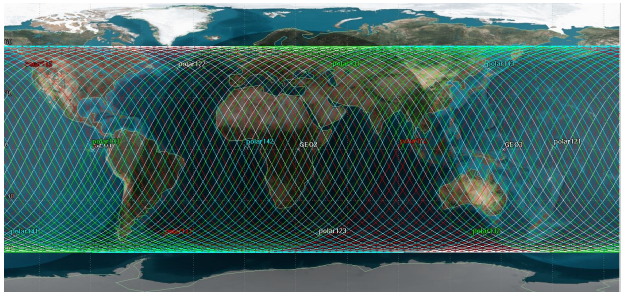

Figure 5: *Ground track of entire LEO constellation after 12 hours.*

4.1.1 Low-Earth Orbit Design

In order to satisfy these requirements, a constellation consisting of twelve satellites are placed in various LEO orbits. The constellation consists of four orbital planes, with three satellites in each. The planes are evenly spaced, differing by 90°, and the satellites are evenly spaced, differing by 120° (Figure 4). As 98 % of all earthquakes occur within $\pm 60°$ latitude, the orbital inclination of the constellation is 60°. The intersection pattern of ground tracks produces satisfactory spatial resolution. (Figure 5).

4.1.2 Low-Earth Orbit Manoeuvres

All LEO spacecraft on the same orbital plane are launched together into an elliptical orbit, with a perigee at 470 km and apogee at 500 km. An separate dispenser is used to circularize the spacecraft's orbits, after which, it performs a de-orbit burn. By timing the insertion manoeuvres of the individual satellites correctly, the difference in orbital periods between the initial and the target orbit is used to achieve the desired separation in true anomaly. The circularisation burn requires 10 m/s of ΔV.

4.1.3 Geostationary Orbit Design

To precisely measure the position of each LEO satellite we use another constellation of three satellite in GEO (Figure 4), separated by 120° in true anomaly such that every LEO satellite can be tracked continuously.

4.1.4 GEO Manoeuvres

Several manoeuvres are required to achieve the above-mentioned constellation. The initial orbit is a Geosynchronous Transfer Orbit (GTO) with a perigee height of 300 km, an apogee height of 35,786 km, and an inclination of 7°. The Low-Thrust propulsion Ion Thruster RIT2X from Airbus is proposed for this purpose, having a specific impulse of 3500 s, providing 88 mN of thrust. The manoeuvre consists of a slow spiral-out thrust pattern, and takes eight months to perform, consuming 1810 m/s of delta-V. Before reaching GEO, two satellites will hold in a slightly-elliptical orbit until their true anomalies reach 120° and 240°, performing circularisation manoeuvres afterwards. Approximately 45 m/s of ΔV is required for yearly station-keeping. The last planned manoeuvre is a transfer to a graveyard orbit, 300 km above GEO, which requires 11 m/s of delta-V.

4.2 Launchers

4.2.1 LEO Launcher

Many launch alternatives are available for micro-satellites, especially to LEO. The most popular method is ride-sharing, which has the advantage of being typically very low cost compared to a dedicated launch. However, ride-sharing is not accurate enough to fulfil the observation requirements. An alternative is the use of micro-launchers. There are over 60 companies providing launch services for small (<350 kg) payloads to LEO. Such a launcher is currently being developed by ArianeGroup. The so-called Q@TS (Quick Access to Space) launcher enables a launch of 100 kg to LEO at a cost of 2 million Euro. This option is chosen for the GRAVL mission.

4.2.2 GEO Launcher

The launcher chosen for GEO satellites is the Ariane 6.2. This results from the fact that at a cost of ca. 75 million Euro, it is the least expensive launcher capable of transferring a 5000 kg payload to GTO. With three satellites of 283 kg, total mass will not exceed 850 kg.

4.3 Primary ISL Ranging Payload

4.3.1 Laser Ranging Principle

From precise measurement of the distance between LEO and GEO spacecrafts, variations in the Earth's gravitational field can be derived. The geometry of the constellation enables a measurement along the gravity acceleration vector. This increases the sensitivity towards gravity anomalies and benefits from an almost isotropic error structure. The distance measurement is done with inter-satellite laser (ISL) ranging. Pulsed laser beams are sent from GEO satellites towards the satellites in LEO, where the beam is reflected. A precise clock on the LEO satellite measures the time-of-flight (TOF) until the laser beam arrives. This measurement principle is outlined in Figure 6. The distance between the GEO and LEO spacecrafts varies between 34,850 km and 37,160 km, which corresponds to 0.2324 s and 0.2478 s. The instrumental requirement that drives the sensitivity of the laser ranging system is that the distance shall be known with a precision of 200 nm/$\sqrt{\text{Hz}}$.

4.3.2 Laser

The laser system design of the GRAVL mission is inspired by the LISA Pathfinder mission, a flight-proven

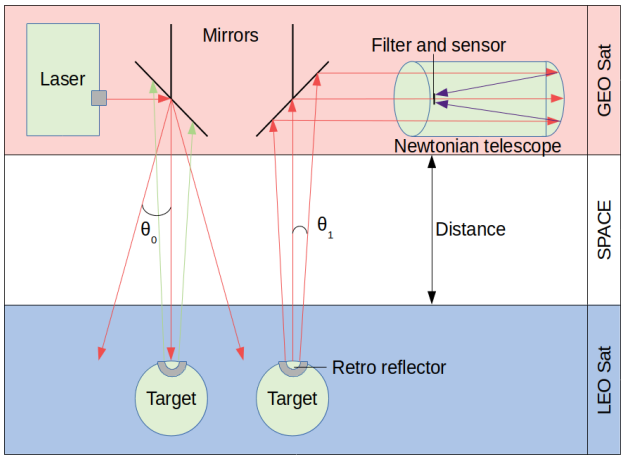

Figure 6: *Transmission path (left) and return path (right) of the inter-satellite laser (ISL) ranging system that is used for distance measurement.*

design with very small divergence angle. This reduces the power need of the GEO spacecraft. The laser divergence is $\theta_0 = 2 \cdot 10^{-5}$ rad. This means that the radius of the laser spot size at LEO is at most 750 m [19, p. 49-50].

4.3.3 Pointing Mirror

The divergence of the laser beam is $2 \arctan\left(\frac{r_{leo\ spot}}{d}\right) \approx 8$ arcsec. In order to enable to target the LEO spacecraft, a high pointing accuracy is required for the mirror.

Each LEO spacecraft is tracked by one GEO spacecraft at a time. The LEO spacecrafts are separated evenly, thus four LEO spacecrafts are tracked by one GEO spacecraft at any given time. Assuming that the pointing mirror can target any desired point within 0.5 s, the exposure is smaller than 0.3 s. This results in a sampling time of $4 \cdot (0.5 + 0.3) = 3.2$ s.

4.3.4 Retro-reflector

Signal transmitted from the GEO satellite will be reflected back by the LEO satellites using retro-reflectors. Each retro-reflector has an acceptance angle of 20° and a radius of 30 mm. In order to provide full 4π coverage, they shall to be distributed every 20° all over the sphere. This ensures that there is always one and only one return beam. Margins exist around these individual zones, and the influence on loss of samples caused by hitting some of these "dead angles" needs to be considered.

It can be seen in Figure 6 that the return angle $\theta_1 < \theta_0$. This is due to the fact that the retro-reflector only reflects back the most collimated part of the incident beam. Using geometrical optics, this implies that the returning beam at the GEO satellite has spot diameter which is twice the diameter of the retro-reflector. By using a large enough mirror, virtually all the reflected photons from the LEO retro-reflector can be captured by the GEO telescope and directed towards the sensor.

4.3.5 Transmitted and Received Power

The laser used in the LISA Pathfinder mission had an output of 2 W. With Equation (3) the power returned by the retro-reflector can be calculated. With a spot radius of 750 m and a retro-reflector radius of 30 mm this results in 80 nW. Depending on the angle of the retro-reflector relative to the laser beam and the distance between the spacecrafts, the returned power is between 74 to 93 nW.

$$P_{return} = P_{output} \frac{\pi \cdot r^2_{retro-reflector}}{\pi \cdot r^2_{LEO\ spot}} \tag{3}$$

4.3.6 Receiver

As stated in the previous section, the Newtonian telescope needs to have an aperture that is larger than the beam from the retro-reflector from the LEO spacecraft. Therefore an aperture of 15 cm is chosen.

The photons get focused into a channel electron multiplier (CEM). The entrance of the CEM has a band-pass filter so that only the 1064.6 ± 0.8 nm from the laser enters the CEM. Each photon that hits the wall gets amplified by secondary electrons that get produced. However, for this instrument a high voltage in the kilo volts is needed. This creates an electric field which has to be shielded from other payloads like antennas.

The charge from the photons and electrons built up at the end of the CEM is measured. The fastest measurement interval is approximately 390 attosecond (117 nm). This is done with sending multiple pulses from the laser in a very short timescale and measuring the harmonics in the signal [20].

4.3.7 Design Considerations

The clock, CEM and comparator need to be mounted as close as possible to each other. This part of the system requires calibration in order to correct for system delays.

Both LEO and GEO spacecraft require precise pointing and position knowledge for accurate ranging and geocoding of data. Positioning will be determined by GNSS receivers which can provide position information with an accuracy of 1 cm. Attitude knowledge shall be provided by combination of both absolute (star trackers) and relative (ring laser gyroscope) measurements.

4.3.8 Feasibility

The main design driver for the laser is the precision required for the ranging system - ranging measurements shall be performed with accuracy within 200 nm in order to achieve required sensitivity. The following components affect the accuracy of the laser ranging

system (estimates for their precision achievable with currently available technologies are included):

- Orientation knowledge of mirror GEO s/c: 0.01 arcsec (2 nm), heritage JWST.
- Orientation knowledge of retro-reflector LEO s/c: 0.5 arcsec (100 nm).
- Clock precision: $1.433 \cdot 10^{-17}$ s (8.6 nm).
- Response laser receiver: $3.9 \cdot 10^{-16}$ s (117 nm).

The sum of these accuracies is 227.6 nm, which is slightly above the 200 nm requirement. Further development and verification is needed to achieve desired accuracy. However, since the discrepancy is relatively low, this improvement is considered achievable.

4.4 Complementary Payload

4.4.1 Accelerometer

The SuperSTAR (Super Space Three-axis Accelerometer for Research mission) accelerometer as flown on GRACE and GRACE-FO has an accuracy of 10^{-10} m/s$^2/\sqrt{\text{Hz}}$ at the precise axes and 10^{-9} m/s$^2/\sqrt{\text{Hz}}$ for the less sensitive axis [21]. Both accuracy and range (10^{-5} m/s^2 and 10^{-4} m/s^2, the latter is for the less sensitive axis) fits the drag accelerations calculated above. Additionally, the instrument measures angular acceleration with a range of $10^{-2}\frac{rad}{s^2}$ (two axes) and $10^{-3}\frac{rad}{s^2}$ (one axis) with a resolution of $5 \cdot 10^{-6}\frac{rad/s^2}{\sqrt{Hz}}$ and $2 \cdot 10^{-7}\frac{rad/s^2}{\sqrt{Hz}}$, respectively. The accelerometer shall be mounted in the centre-of-mass (CoM) of the spacecraft.

4.4.2 GNSS Receiver

In order to determine accurate location of the LEO spacecraft, an OEM719 GNSS receiver could be used. The GNSS measurement makes use of multitude of frequencies, on up to five channels. While the stated accuracy is only a few meters, post-processing of the GNSS satellite signal on the ground can improve it to a precision of a few centimetres. Therefore, the GNSS signal is sampled and stored in spacecraft memory and downlinked later to the ground. Each GNSS data package consists of a 1023-bit string. The GNSS time signal will be used to time-stamp the other on-board measurements.

4.4.3 ADS

Orientation of the LEO spacecraft with respect to the incident laser beam needs to be known with high precision, to compensate for shift of the retro-reflector along the beam direction. For this, a high-precision attitude determination system (ADS) has to be used on the LEO s/c. The main elements of the system are star trackers and gyroscopes. With information on both attitude and rotation, statistical attitude determination can be included in the data post-processing. Additionally, the GNSS time signal can be used to optimise the GEO-LEO range reconstruction with attitude information. The LEO s/c is also equipped with magnetorquers, in order to damp spacecraft rotation when needed, further improving the statistical attitude reconstruction.

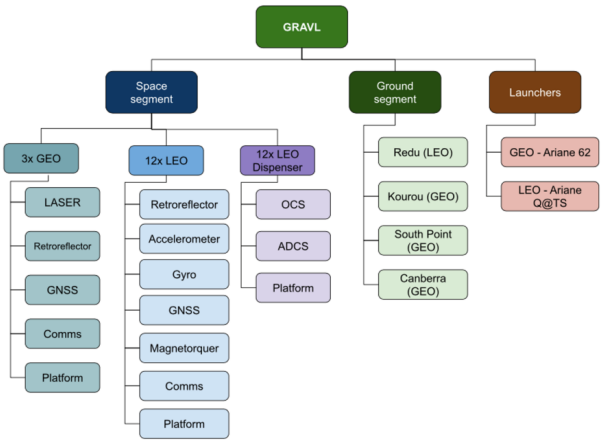

Figure 7: *Overview of GRAVL measurement system with the most important payloads for the GEO (turquoise), LEO (blue) s/c and the LEO dispensers (purple), as well as the ground segment (green) and launchers (red).*

5 Space Segment

5.1 System Overview

The GRAVL measurement system consists of ground segment, space segment and launchers. The space segment comprises 12 LEO satellites, three GEO satellites and dispenser stages for LEO constellation phasing and orbit insertion. The ground segment includes ground stations for GEO satellites and also for LEO constellation. The system overview is presented in Figure 7.

5.2 GEO Satellite Design

The GEO system design is driven by scientific mission goals and reliability requirements.

A highly reliable satellite platform selection is driven by 7 year mission lifetime. The GEO satellites have high demands regarding environmental and mechanical sustainability as well as for spacecraft mass, size and power generation. Such performance cannot be achieved by components designed for nano-satellites. Due to the mentioned aspects, a larger satellite platform shall be used that is designed and qualified for GEO. The same requirement applies for the on-board components. Suitable platforms are available and here Airbus/Astrium is selected as platform provider, as the company has long experience in GEO missions and a large portfolio of GEO spacecraft components. Only

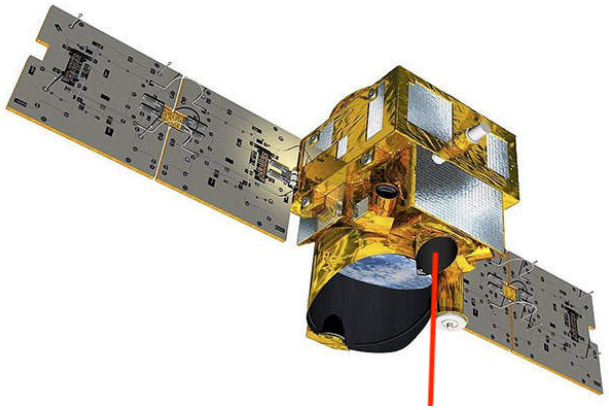

Figure 8: *MERLIN active laser remote sensing mission using Airbus/Astrium AstroBus-S spacecraft.*

GEO qualified components can provide the required quality, performance, and guaranteed life-time for the planned mission at a competitive price.

The Airbus/Astrium AstroBus-S spacecraft platform (Figure 8) is selected as baseline for the GEO spacecraft. The platform comes with a required size of $100 \cdot 100 \cdot 170$ cm^3, equipped with full suite of on-board components for bus operation. The s/c itself has a cubic shape with one large opening/baffle for the laser ranging system. Solar panel wings are mounted onto two sides of the spacecraft.

The system architecture is divided into a main bus and a payload segment. The main bus is used during LEOP, orbit maintenance and nominal scientific operation. The payload systems are switched on for science data retrieval. The s/c main bus consists of an on-board computer, attitude control and determination system, clock control and management system, an interface module and various support equipment. The payload subsystem consists of an atomic clock and the laser ranging system.

5.3 LEO Micro-satellite Design

The laser-tracked retro-reflector spacecraft in LEO can be considered gravity field probes that provide science data, i.e. their precise position, measured with extreme accuracy in the radial direction of gravity field. The measurement is carried out by laser ranging and therefore the satellite is covered by laser corner retro-reflectors, spaced in the way that only one retro-reflector is ever seen by a GEO spacecraft at a time. Precision is enabled by mitigation of non-gravitational effects and computational compensation of residual perturbations. The latter requires only knowledge about disturbances, while mitigation reduces the effects by design.

The main effects that can be reduced by design are of aerodynamic and thermal nature. Therefore, the satellite architecture is based on a solid spherical metal body that guarantees a very high mechanical stiffness and reduces thermal deformation and atmospheric drag. The satellite design is driven by ballistic properties and symmetry, driven by lack of active attitude control during measurement. Therefore, the retro-reflectors, GNSS antennae, communication antennae and other sensors are distributed over satellite surface evenly. Knowledge of residual drag is acquired via a high-precision accelerometer. Using this data, the drag-induced acceleration can be eliminated from measurements. The stability is further improved by using only passive components to prevent micro-vibrations caused by moving parts.

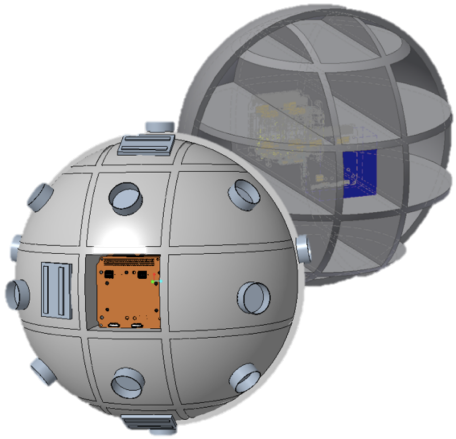

Figure 9: *Concept design of LEO s/c, with GNSS antennae and retro-reflectors is shown (on purpose exaggerated). The rest of the sphere shall be covered in solar panels.*

The sphere walls and inner plates of the structure provide much higher radiation shielding, thermal capacity, and thermal conductivity than typical nano-satellites and the high mass reduces the effect of drag.

The s/c is equipped with a set of high precision sensors. The sensors are described in Table 3.

Table 3: *Sensors on the LEO platform.*

Pcs	Sensor	Type	Details
3	Magnetometer	rel.	0.1 μT resolution
1	Gyroscope	rel.	AWR 0.0035°/h
4	Horizon detector	rel.	<1° accuracy
4	GNSS receiver	abs.	L1/L2, 5 channels
4	Startracker	abs.	5 arcsec accuracy

The antennae have a 3 dB beam width of 60°. The entire surface is covered as evenly as possible with antennae, retro-reflectors and solar panels. Figure 9 shows a CAD model of the LEO s/c.

Because the position is in fact level 1 science data, GNSS antennae and receiver are considered payload components rather than navigation. Using multiple GNSS (with the novelty of GALILEO on-orbit) and multi-channel receivers, an accuracy in the order of magnitude of 10 mm can be achieved, which allows

precise orbit determination and is required for the gravity field retrieval.

5.4 Mission Timeline

Should the proposal be accepted, the mission analysis, feasibility review, preliminary definition and detailed definition phases need to follow, each lasting roughly one year. Near the end of the detailed definition phase, the satellites can begin production and testing, including vibration and thermal-vac testing for all 48 LEO satellites and 3 GEO satellites. Earliest possible start of operations is estimated to mid-2025. Utilisation can commence once all three GEO satellites and first generation of twelve LEO satellites is launched.

Due to lifetime limitations of the LEO satellites, a new set of twelve LEO satellites is launched every two years, for a total of 3 constellation refreshes. The LEO satellites will naturally de-orbit within 5.2 years (Subsection 6.3), opening the possibility for extended measurements at decreasing altitudes.

5.5 Ground Segment

Daily data production for GEO satellites has been estimated at 50 MB per day. The GEO satellites remain in one location in the sky all day and thus downlink can occur at any time of day. They are distributed evenly above the equator, which means that the mission will require use of three different ground stations in ESA's Estrack expanded network. The chosen stations are Kourou, South Point, and Canberra.

Each LEO satellite will pass over the 2.6-m S-band antenna at the Redu ground station in Europe at least once per day, and can downlink all of its data (<10 MB) within a few seconds.

6 Programmatics

6.1 Cost Estimation

The overall cost of the mission is estimated at approximately 380 million Euro. The GEO launcher represents the most expensive single item at 75 million Euro. Each launch of a LEO satellite is estimated to cost 3 million Euro, resulting in a total LEO launch cost of 48 million Euro. The GEO satellites cost approximately 20 million Euro, the LEO satellites 1.4 million Euro. Overall operations of the mission are estimated to cost 25 million Euro over seven years.

6.2 Risks

The risks associated with the mission implementation have been evaluated. One of the most critical technologies required for this mission is high performance laser ranging. However, with sufficient investment the performance can be reached as demonstrated by LISA pathfinder mission. The mission competitive price relies on availability of microlaunchers, currently under development. In case of non-availability of the microlauncher, more expensive launches might be required. Moreover, there is also risk related to occurrence probability of earthquakes. Three decades are needed in order to differentiate between the secular changes of natural mass redistribution and the earthquake ones if the sources are close. The obvious mitigation would be to increase the lifetime of the mission.

Table 4: *Power, mass, cost, Δv, and data budgets for the three different s/c.*

Spacecraft	GEO platform	LEO platform	LEO dispenser
Req. (avail.) power [W]	545.66 (2114.58)	33.20 (40.38)	136.42
Mass [kg]	283.49	27.47	8.28
Cost [M €]	20.22	1.38	0.28
Δv [m/s]	2136.00	-	20.00
Data [Mbit/day]	47.30	3.24	-

6.3 Space Debris Mitigation

Recognising the responsibility towards future space-faring generations, GRAVL will be in compliance with ESA's space debris mitigation (SDM) guidelines [22]. The LEO s/c will de-orbit after 3 to 5.2 years. An even shorter lifetime is expected for the Q@TS upper stage. Finally, the satellite dispensers will de-orbit actively. The three GEO s/c have a foreseen lifetime of 7 years and will transfer to a graveyard orbit 300 km above GEO. The upper stage of Ariane 6.2 performs active de-orbiting.

At the end of the life (EOL) of all s/c, the pressure vessels are depleted, batteries discharged and active rotating components go into a no-collision mode. This means that our mission complies with requirement 6.3.2.2 and 6.2.2.3 of the SDM guidelines [22, p. 20-25].

7 Discussion

The primary science objective of this mission is to observe mass redistribution in the upper mantle before, during, and after seismic events. This requires temporal and spatial resolutions of 3 days and 100 km, respectively. Achieving such requirements can only be achieved by measuring the vertical component of the gravity field. This is accomplished by measuring the vertical deviations in the orbital trajectories of satellites in LEO from platforms in GEO. This places a high demand on the laser ranging accuracy: 200 nm. Non-gravitational forces perturbing the LEO spacecraft need

to be accurately accounted for to further reduce the sensitivity. In addition, the detector needs to be developed from a TRL of 4 to flight-readiness. The spherical shape of the LEO spacecraft with retroreflectors is an innovative development in measurement, which has the advantage of requiring minimal control and a high ballistic coefficient.

8 Conclusion

We propose GRAVL for consideration as a future ESA mission, since it provides the opportunity to significantly improve understanding of geophysical processes and of the Earth's interior, by providing data about Earth's mass distribution with unprecedented spatial and temporal resolution. Earthquakes have severe economic and societal impact, and improvement of seismic models can aid in their monitoring and risk mitigation processes in seismically active areas.

Bibliography

[1] Chao *et al.*, "Gravity changes due to large earthquakes detected in GRACE satellite data via empirical orthogonal function analysis", *Journal of Geophysical Research: Solid Earth*, 2019.

[2] D. C. Agnew, "Variable star symbols for seismicity plots", *Seismological Research Letters*, 2014.

[3] Agnew *et al.*, "Variable Star Symbols for Seismicity Plots", *Seismological Research Letters*, 2014.

[4] Bondár *et al.*, "ISC-GEM: Global instrumental earthquake catalogue (1900–2009), ii. location and seismicity patterns", *Physics of the Earth and Planetary Interiors*, 2015.

[5] Kostoglodov *et al.*, "A large silent earthquake in the Guerrero seismic gap, Mexico", *Geophysical Research Letters*, 2003.

[6] M. Drinkwater *et al.*, "GOCE: Obtaining a portrait of Earth's most intimate features", 2008.

[7] B. D. Tapley, S. Bettadpur, J. C. Ries, P. F. Thompson, and M. M. Watkins, "GRACE measurements of mass variability in the earth system", *Science*, vol. 305, no. 5683, pp. 503–505, 2004.

[8] Panet *et al.*, "Upper mantle rheology from GRACE and GPS postseismic deformation after the 2004 Sumatra-Andaman earthquake", *Geochemistry, Geophysics, Geosystems*, vol. 11, no. 6, 2010.

[9] Panet and others, "Migrating pattern of deformation prior to the Tohoku-Oki earthquake revealed by GRACE data", *Nature Geoscience*, 2018.

[10] A. Bacchetta *et al.*, "From GOCE to NGGM: Automatic control breakthroughs for European future gravity missions", *IFAC-PapersOnLine*, 2017.

[11] Hauk *et al.*, "Gravity field recovery in the framework of a Geodesy and Time Reference in Space (GETRIS)", *Advances in Space Research*, 2017.

[12] M. Hauk and R. Pail, "Gravity field recovery using high-precision, high–low inter-satellite links", *Remote Sensing*, vol. 11, no. 5, 2019.

[13] Pail *et al.*, "Science and user needs for observing global mass transport to understand global change and to benefit society", *Surveys in Geophysics*, 2015.

[14] Visser *et al.*, "Towards a sustained observing system for mass transport to understand global change and to benefit society", in *Fourth Swarm Science Meeting & Geodetic Missions Workshop*, 2017.

[15] Rogers *et al.*, "Episodic tremor and slip on the Cascadia subduction zone: The chatter of silent slip", *Science*, 2003.

[16] Gaias *et al.*, "Model of J2 perturbed satellite relative motion with time-varying differential drag", *Celestial Mechanics and Dynamical Astronomy*, 2015.

[17] The Committee on Space research (COSPAR), *COSPAR International Reference Atmosphere (CIRA-2012)*, 2012.

[18] K. F. Wakker, *FUNDAMENTALS OF ASTRODYNAMICS*. Institutional Repository Library Delft University of Technology Delft - The Netherlands, 2015.

[19] K. Danzmann *et al.*, "Lisa: Laser interferometer space antenna", Institut für Atom- und Molekülphysik, Tech. Rep., 1998.

[20] Zhang *et al.*, "Full characterization of an attosecond pulse generated using an infrared driver", *Nature*, 2016.

[21] J. Flury, S. Bettadpur, and B. D. Tapley, "Precise accelerometry onboard the GRACE gravity field satellite mission", *Advances in Space Research*, 2008.

[22] ESA, "ESA space debris mitigation compliance verification guidelines", 2015.